Male gut microbiome mediates post-mating sexual selection in *Drosophila*

Komal Maggu*, Abhishek Meena, Alessio N. De Nardo, Sonja H. Sbilordo, Jeannine Roy & Stefan Lüpold*

Department of Evolutionary Biology and Environmental Studies, University of Zurich, Winterthurerstrasse 190, 8057 Zurich, Switzerland

Correspondence: komal024maggu@gmail.com, stefan.luepold@uzh.ch

ABSTRACT

In polyandrous systems, male reproductive success is critically influenced by sperm competition, a process often mediated by ejaculate characteristics that are sensitive to male condition. While condition dependence is a cornerstone of sexual selection theory, the role of the gut microbiome in modulating male reproductive fitness under sperm competition remains unexplored. Here, we investigated the impact of varying gut microbial compositions on sperm competitive ability in *Drosophila melanogaster*. By inoculating germ-free (axenic) males with all 32 full-factorial combinations of five common commensal bacteria, we demonstrated that the presence and diversity of commensal gut microbes significantly enhance male sperm offense ability. Specifically, males associated with a more diverse microbiota exhibited superior competitive fertilization success, accompanied by increased sperm transfer, higher sperm viability, and a greater proportion of sperm stored by females. Predictive models further revealed complex, non-additive interactions among bacterial species in their effects on sperm competitiveness. These findings suggest that the gut microbiome acts as a critical modulator

of male reproductive fitness, challenging traditional models of sexual selection that overlook contributions of non-pathogenic bacteria to condition-dependent traits.

INTRODUCTION

In polyandrous species, where females mate with multiple males, sperm competition often determines fertilization success based on ejaculate size and quality (1, 2). However, producing large, high-quality ejaculates is costly by diverting resources from other fitness traits (3–7). The dependence of trait expression on resource availability and allocation between growth, maintenance, and reproduction is central to sexual selection theory, linking phenotypic quality to underlying genetic variation: traits that reliably indicate a male's ability to acquire and allocate limited resources are hypothesized to signal heritable fitness benefits to mates or rivals (8, 9). This 'good genes' framework assumes that male condition is shaped by genetic variation in resource acquisition, allocation efficiency, or stress tolerance (10, 11). However, the gut microbiome – a dynamic microbial consortium known to modulate host nutrient extraction, metabolic regulation, and hormone synthesis (12, 13) – represents a potent, yet unexplored, factor that could decouple male condition from host genetics. Critically, by independently modulating host resource budgets, microbial communities could fundamentally alter the heritability of condition-dependent traits, thereby challenging a cornerstone of sexual selection theory.

The gut microbiome directly modulates host physiology, including nutrient assimilation (14–16), energy allocation (17–19), and hormone signalling (20), which collectively can influence reproductive function. Indeed, across diverse taxa, microbiome composition is well-documented to shape female reproductive biology (17, 21, 22), with functional differences between key bacterial groups (e.g., *Acetobacter* vs. *Lactobacillus* in *Drosophila*) influencing

50 metabolic and fecundity outcomes (17, 23). By contrast, the role of the gut microbiome in male
51 reproductive fitness, particularly its impact on fertilization success under sperm competition,
52 remains entirely unexplored, despite limited associations between dysbiosis and impaired
53 testicular function(24, 25) or between seminal microbes to sperm motility (26, 27).

54 Here, we tested the hypothesis that the gut microbiome modulates male reproductive
55 fitness under competitive fertilization by enhancing condition-dependent ejaculate traits in
56 *Drosophila melanogaster*, a model for tractable host-microbe interactions (28, 29).
57 Specifically, we inoculated males with all 32 full-factorial combinations of five gut bacteria
58 (*Acetobacter orientalis*, *A. tropicalis*, *A. pasteurianus*, *Lactobacillus brevis*, and *L. plantarum*).
59 When present together, these species recapitulate key phenotypic traits of flies with intact
60 microbiomes (Supplementary Fig. 1) and represent bacteria with established roles in female
61 fitness (17). We then quantified competitive fertilization success (P_2) and its mechanistic
62 underpinnings: sperm viability, transfer, and storage. We predicted that (i) males with diverse
63 microbiomes outperform axenic (i.e., germ-free) or low-diversity males due to improved
64 nutrient acquisition (14, 30), (ii), competitive advantages are amplified by bacterial identity
65 (e.g., *Acetobacter* abundance), synergistic interactions, and community composition (e.g.,
66 *Acetobacter*-dominance) (17), and (iii) microbiome-driven gains in sperm viability, transfer
67 efficiency and competitive storage underpin fertilization success (31, 32). By resolving how
68 microbial communities shape sperm competition, this study bridges microbial ecology with
69 sexual selection theory, offering novel insights into the evolution of condition-dependent traits.
70

71 **RESULTS AND DISCUSSION**

72 **Microbial diversity enhances sperm competitiveness**

73 To test if gut microbes influence male reproductive fitness under post-mating sexual selection,
74 we compared the competitive fertilization success of male *D. melanogaster*, inoculated with

75 gut bacteria in all possible combinations between our five strains, using a full-factorial
76 combinatorial approach (32 consortia) validated through colony morphology and 16S
77 sequencing (Methods, Supplementary Figs. S1 and S2). This combinatorial design—building
78 on established gnotobiotic methodologies (17) but applied here to sperm competition—enabled
79 high-resolution dissection of species interactions mediating host phenotypes. Standard
80 competitor males (either axenic or conventional with intact microbiomes), which ubiquitously
81 expressed green fluorescent protein (GFP) for paternity assignment (32, 33), mated three days
82 before focal wild-type males, thereby providing distinct competitive contexts to resolve
83 intrinsic microbiome benefits.

84 In competition against axenic rivals, we found experimental males harbouring any single
85 bacterial species (except *L. brevis*) or consortium to outperform males without a microbiome,
86 with second-male paternity (P_2) increasing with species richness (generalized linear mixed
87 models (GLMM) repeated across 1,000 bootstrapped datasets, accounting for block, microbial
88 combination and overdispersion: $N = 646$ across 32 microbial combinations: odds ratio, $OR =$
89 1.09 [95% confidence limits: 1.00, 0.15]; Fig. 1A). Being associated with all five species
90 translated into a 27% gain in P_2 compared to the axenic state (mean proportion ± s.d. = 0.85 ±
91 0.05 vs. 0.67 ± 0.05, respectively). These patterns persisted when focal males competed against
92 rivals with intact (unmanipulated) microbiotas [increase with richness: $N = 624$, $OR = 1.05$
93 [1.00, 1.10]; relative gain for 5-species association: 20% (0.72 ± 0.08 vs. 0.60 ± 0.03)],
94 confirming that microbiome benefits reflect intrinsic physiological enhancement rather than
95 competitor compromise.

96 This reproductive deficit in axenic males aligns with established connections between
97 microbiome absence and physiological dysregulation in *Drosophila* (34). Such microbial
98 modulation of condition dependence likely extends beyond *Drosophila*, as gut microbiomes
99 influence nutrient assimilation across the animal tree of life. While our study did not directly

100 assay host metabolic states, prior work compellingly shows that axenic flies often exhibit
101 hyperlipidemia and impaired insulin signalling – conditions detrimental to overall health and
102 potentially sperm function (35, 36). These metabolic disturbances can be rescued or modulated
103 by specific gut bacteria; for example, *Acetobacter* species are known to restore lipid
104 homeostasis, potentially via acetate production (37) (which may protect against sperm
105 oxidative damage), whilst certain *Lactobacillus* species exacerbate oxidative stress (38), which
106 can directly compromise sperm membranes and DNA integrity (39). In fact, *Acetobacter*-
107 dominated communities conferred greater benefits than those biased toward *Lactobacillus*,
108 regardless of the standard competitor (Fig. 2A). The contrasting impacts of *Acetobacter* and
109 *Lactobacillus* on P_2 based on their presence and absence were further supported by
110 bootstrapped correlations between P_2 and the relative abundances (based on CFU counts) of
111 each species across different microbial communities. These correlations yielded consistently
112 positive and negative covariation with *Acetobacter* and *Lactobacillus* species, respectively,
113 indicating a more quantitative pattern than sole presence or absence (Fig. 3A).
114 Combined, although our results establish that microbial diversity and particularly
115 *Acetobacter* dominance directly enhance male competitive fertilization success, challenging
116 classical frameworks attributing condition dependence solely to host genetics and resource
117 status or stress resilience (11).
118
119 **Microbial interactions shape competitive outcomes**
120 Bootstrapped generalized linear mixed-effects models (GLMMs), controlling for experimental
121 block, indicated that microbial interactions—rather than additive effects—were the primary
122 drivers of variation in P_2 across the 32 microbial consortia. There was no strong evidence for a
123 five-way interaction among bacterial strains in sperm competition against either axenic males
124 (N = 646, OR = 0.82 [0.55, 2.66]) or conventional rivals (N = 624, OR = 0.76 [0.40, 1.39]).

125 However, after excluding these highest-order interactions, there was a clear four-way
126 interaction among *At* × *Ap* × *Lb* × *Lp* in competitions against axenic males (*OR* = 1.84 [1.22,
127 2.77]) and among *Ao* × *Ap* × *Lb* × *Lp* in those against conventional males (*OR* = 0.67 [0.49,
128 0.93]), suggesting complex microbial effects on reproductive outcomes. Additionally, two and
129 four three-way interactions, as well as six and eight of the ten two-way interactions had
130 bootstrapped confidence intervals that excluded zero between the two models, respectively,
131 further supporting a non-additive contribution of microbial composition (Supplementary Figs.
132 S2 and S3).

133 Predictive modelling showed that averaging mono-association effects between bacterial
134 strains poorly forecasted outcomes for multi-species communities (e.g., mean of *At*, *Ap*, and
135 *Lb* to predict the *At-Ap-Lb* combination), with only eight (30.8%) of the 26 possible
136 combinations correctly predicted based on 95% confidence intervals including zero difference
137 in competitive matings against axenic rivals (Fig. 2B). Averaging pairwise combinations to
138 predict three-way species interactions (e.g., *At-Ap*, *At-Lb* and *Ap-Lb* to predict *At-Ap-Lb*)
139 indicated similar accuracy (31.2%: 5 of 16 predicted combinations; Fig. 2B). These predictions
140 by mono- or di-associations were broadly comparable when focal males competed against
141 conventional rather than axenic first males (33.0 and 37.5%, respectively).

142 Additionally, pairwise interactions were context-dependent, varying conditionally on the
143 remaining ("bystander") species as reflected by interactions trending from positive
144 (synergistic) to negative (antagonistic) between the same two species depending on the
145 configuration of additional species in the microbiota (Fig. 4A). This dependence on bystanders
146 also held for three-way interactions between focal species (Fig. 4B). The prevalence of these
147 non-additive effects reveals that microbial consortia function as integrated units—not mere
148 sums of parts—mirroring ecological dynamics in host-microbe systems (40). Such complexity
149 suggests microbiome stability itself could be a target of sexual selection, with selection

150 favouring host genotypes that stabilize high-performance communities (e.g., *Acetobacter*
151 dominance), potentially explaining a microbiome-mediated resolution of the lek paradox (41).
152

153 **Mechanistic basis of microbiome-mediated fitness**

154 To dissect how microbiomes enhance competitive fertilization success, we quantified sperm
155 transfer, sperm viability, and female sperm retention and storage patterns, based on prior
156 knowledge (31–33, 42). Due to the similar results between axenic and conventional competitor
157 males, we here restricted our mechanistic investigation to axenic first males. For visualization
158 of sperm, all assays except sperm viability involved standard and experimental males that,
159 respectively, expressed green or red fluorescent protein in sperm heads (43).

160 We found that a more diverse microbiome directly translates into improved ejaculate
161 quality, providing the mechanistic basis for enhanced competitive fertilization success (Fig. 1).
162 While axenic and mono-associated focal males transferred similar sperm quantities (Figs. 1B
163 and 2C), multi-associated males transferred 3–36% more sperm than either of the former
164 categories, with gains scaling with microbial diversity (bootstrapped linear mixed model
165 (LMM) controlling for block and microbial combination: $N = 582$, $\beta = 57.14$ [40.68, 76.47];
166 Figs. 1B and 2C,D). Sperm viability also increased with diversity: males with all five species
167 had 94.9 ± 2.3% viable sperm compared to 54.5 ± 6.5% in axenic males (GLMM: $N = 320$, OR
168 $= 1.62$ [1.52, 1.71]; Figs. 1C and 2E, F). Critically, freshly remated females tended to delay the
169 ejection of displaced and excess sperm from first (standard) and second (experimental) males,
170 respectively, if second males were associated with a more diverse microbiome (LMM: $N =$
171 582, $\beta = 3.73$ [-0.09, 7.39; 90%CI: 0.45, 6.90]; Figs. 1D and 2G,H), thereby increasingly
172 biasing sperm storage toward these males (GLMM on relative sperm numbers in storage: $N =$
173 582, $OR = 1.40$ [1.34, 1.46]; Figs. 1E, 2I,J). Hence, microbiome-enhanced sperm quality or
174 displacement efficiency biased post-mating sperm storage dynamics. Confirming prior work

175 (31–33, 42), the relative numbers of sperm stored and their viability covaried with paternity
176 outcomes (Fig. 3B). Further, these phenotypic traits again covaried mostly positively with
177 *Acetobacter* and negatively with *Lactobacillus* when considering relative colony forming units
178 (CFUs) rather than species presence or absence (Fig. 3A).

179 Similar to P_2, the component traits underlying competitive fertilization success were
180 shaped by higher-order microbial interactions. Bootstrapped GLMMs revealed significant five-
181 way interactions for both sperm viability ($N = 320$, $OR = 0.29$ [0.13, 0.63], Supplementary Fig.
182 S4) and the proportion of second-male sperm stored by females ($N = 582$, $OR = 2.34$ [1.38,
183 4.11], Supplementary Fig. S5). We detected a comparable five-way interaction in an LMM for
184 time to female sperm ejection ($N = 582$, $\beta = 150.10$ [41.74, 255.22], Supplementary Fig. S6).
185 While no five-way interaction was found for the number of sperm transferred, a consistent
186 four-way interaction among *Ao* × *Ap* × *Lb* × *Lp* emerged ($N = 582$, $\beta = 393.09$ [198.49,
187 582.51], Supplementary Fig. S7), with nearly all two- and three-way interactions also showing
188 effect distributions shifted away from zero. Predictive models also indicated considerable
189 underestimation of observed values for sperm viability and relative sperm storage when using
190 additive models based on mono- or di-associations (Fig. 2F,J), highlighting the importance of
191 higher-order interactive effects. This dependence on microbial context appeared weaker for
192 both the number of sperm transferred and time to sperm ejection. Across all stages of the
193 competitive fertilization process, interactions among microbial pairs or triplets were often
194 modulated by the presence of additional "bystander" species, emphasizing the context-
195 dependent nature of microbial effects (Fig. 4C–J).

196

197 **Evolutionary implications**

198 The observed improvements in ejaculate quality and subsequent P_2 gains conferred by species-
199 rich microbial communities likely stem from their ability to restore or optimize host metabolic

200 homeostasis and nutrient allocation toward reproduction. The superior performance associated
201 with *Acetobacter*-dominated communities (Fig. 1) lends support to this hypothesis, given their
202 known efficacy in nutrient assimilation and influencing host metabolism (34). These microbes
203 may channel resources more effectively towards energetically costly ejaculate production and
204 maintenance, potentially mitigating damage from metabolic byproducts. However, the
205 significant non-additive effects underscore that the *integrated function* of the microbial
206 consortium, rather than simply the presence of key species, dictates the ultimate physiological
207 impact (Fig. 3). Although metabolite-specific mechanisms await future study, our reductionist
208 approach definitively isolates microbiome contributions to sperm competitiveness.

209 Our findings prompt a re-evaluation of core tenets in sexual selection theory. By acting
210 as an amplifier of condition-dependent reproductive traits, the microbiome introduces
211 complexity to the "good genes" model, where such traits are assumed to reliably signal host
212 genetic quality (10, 11). Our results suggest that the microbiome functions as a "hidden
213 mediator," bridging host genetics and environmental inputs (44), with at least three key
214 evolutionary implications.

215 First, the microbiome potentially introduces a transmissible component influencing
216 fitness that is sensitive to environmental factors (diet, social context) and operates outside strict
217 Mendelian inheritance (44). If microbial consortia are consistently acquired or partially
218 transmitted (vertically or horizontally), this could contribute to maintaining heritable variation
219 in sexually selected traits, offering a potential factor in resolving the lek paradox (41).
220 Furthermore, the microbiome might act as an "environmental sensor," allowing males to buffer
221 reproductive output against nutritional fluctuations (7), thereby stabilizing their fitness.

222 Second, the context-dependent microbial interactions (Fig. 3) and potential trade-offs
223 (e.g., benefits vs. costs like oxidative stress potentially associated with *L. brevis*) suggest
224 complex coevolutionary dynamics. Selection may favour host mechanisms for managing

225 microbial partners ("screening" or selectively retaining beneficial symbionts), while microbes
226 may adapt to host environments, potentially leading to conflicts or mutualisms influencing
227 reproductive outcomes(45).

228 Third, the influence of the microbiome clearly extends into the female reproductive tract.
229 The finding that females preferentially stored sperm from males with more diverse
230 microbiomes (Figs. 1E and 2I) strongly suggests that microbiome-mediated enhancements to
231 ejaculate quality (sperm function and viability, possibly seminal fluid composition) interact
232 with female physiological processes. This opens a potential new dimension for cryptic female
233 choice (46, 47) with selection acting on microbiome-influenced male phenotypes. Critically,
234 while our *Drosophila* model provides mechanistic tractability, microbiome-mediated condition
235 dependence likely operates universally where sperm competition occurs.

236 The prevalence of synergistic effects also suggests that microbiome complexity and
237 functional integration might themselves be targets of selection, favouring males capable of
238 harbouring stable, high-performing microbial communities. Mechanistically, this could
239 involve selection for host factors that influence microbial colonization, resource availability
240 within the host environment, or the establishment of specific microbial interactions. Males with
241 genotypes promoting a harmonious and efficient microbial ecosystem would likely experience
242 enhanced physiological performance, ultimately translating to greater reproductive success.

243

244 **Towards microbiome-integrated sexual selection**

245 Realizing a comprehensive, microbiome-aware framework for sexual selection necessitates
246 several key avenues of future research. Foremost among these is the need to elucidate the
247 precise functional mechanisms underlying the observed fitness effects. This will require
248 integrated 'omics' approaches (e.g., metabolomics, proteomics, transcriptomics) to map the
249 links between microbial communities, their metabolites, and key ejaculate features influencing

fertilization success. Alongside understanding the functional basis, it is also critical to determine how these fitness-enhancing microbiotas are maintained within populations. Future studies should therefore quantify the relative importance of different routes of transmission—including vertical passage, coprophagy, social interactions, or seminal transfer—and assess the stability, or heritability in a broad ecological sense, of beneficial microbial consortia across generations and varying environmental conditions.

Furthermore, exploring the role of females in these interactions would be an important avenue for future research. Investigations should examine female biases in both pre- and post-mating choice relative to potential male microbial cues or the enhanced quality of ejaculates produced by microbiome-rich males. A particularly crucial, yet unexplored, aspect is whether the female's own resident microbiome interacts with the incoming ejaculate or associated microbes, potentially influencing sperm storage patterns and biasing competitive outcomes independently of male traits.

Finally, the ecological context and broader applicability of our findings require exploration. While host-manipulation becomes increasingly challenging in systems with richer microbiotas, our full-factorial study established core principles of microbial interaction hierarchies that likely scale to complex communities. Research should examine how diet-microbiome interactions shape male reproductive strategies under varying resource conditions. Critically, assessing generality in species with diverse mating systems and modes of microbial transmission will reveal the evolutionary scope of these interactions. Although natural microbiomes generally exceed five species, functionally defined 'guilds' (e.g., acetate-producers) can be modelled combinatorially. Given deeply conserved microbiome functions across taxa, our framework provides a blueprint for targeted manipulation of keystone interactions in other tractable systems.

275 **Conclusion**

276 Our research demonstrates that the gut microbiome is an active participant in shaping male
277 reproductive competitiveness. By influencing ejaculate quality and quantity, likely through
278 modulation of host metabolism and resource allocation(7, 48, 49), these microbial symbionts
279 redefine the landscape of condition dependence. Integrating the microbiome into sexual
280 selection theory may fundamentally alter our understanding of how fitness variation is
281 generated, maintained, and acted upon by selection in polyandrous systems and beyond. Our
282 study emphasized the importance of considering the hologenome—the host plus its associated
283 microbiota—as the relevant unit of selection when investigating the evolution of complex
284 reproductive traits.

285

286

287 **MATERIAL AND METHODS**

288 **Experimental populations**

289 Throughout this study, we used *Drosophila melanogaster* of the LH_m strain. These were either
290 derived from an outbred wild-type population or, for standard competitors in the sperm
291 competition assay, from a backcrossed population that had been genetically modified to
292 ubiquitously express green fluorescent protein (GFP), permitting paternity assignment against
293 the focal wild-type males (32, 33). To study biases in female sperm storage, we used focal
294 males whose sperm heads expressed red fluorescent protein (RFP), and our standard
295 competitors with ubiquitous GFP expression, permitting quantification of each competitor's
296 sperm inside the female reproductive tract (32, 33, 43). We maintained all fly populations at
297 moderate densities under constant conditions of 25°C, 60% humidity, and a 12h:12h light:dark
298 cycle.

299

300 **Generating axenic flies**

301 To generate axenic flies, we performed all steps hereafter in a laminar flow chamber to avoid
302 contamination. First, we collected eggs from Petri dishes containing grape-juice agar with a
303 smear of yeast paste that had been placed in four large population cages after a six-hour egg-
304 laying period. After washing these eggs off the plates into a strainer, we dechorionated them
305 with 3.5% bleach for 2 minutes, followed by a rinse in 70% ethanol and three rinses with sterile
306 water. We then transferred these eggs to autoclaved standard fly food supplemented with
307 antibiotics (ampicillin, kanamycin, erythromycin, and tetracycline at final concentrations of
308 50, 50, 10, and 10 μg/ml, respectively) in autoclaved glass vials. These vials were then left
309 undisturbed under standard conditions for flies to develop.

310 Upon fly eclosion, we collected both males and females as virgins, separated them by
311 sex and confirmed their axenic state by plating a homogenized subsample of flies on LB and
312 MRS agar followed by 16S PCR. Briefly, we extracted genomic DNA from 3−5 pooled axenic
313 flies per sample using the ZymoBiomics™ DNA Microprep kit following the instructions
314 provided by the manufacturer. We also extracted DNA from flies with an intact microbiome to
315 serve as positive controls. For DNA amplification, we used bacterial universal primers 27F and
316 1492R as forward and reverse primers, respectively. We prepared the PCR master mix using
317 9.5 μl of nuclease free water, 12.5 μl kappa HiFi master mix, 1 μl of forward and reverse primer
318 and 1 μl of template DNA. The PCR cycle included an initial denaturation at 95°C for 90 s,
319 followed by 35 cycles of denaturation at 95°C for 30 s, annealing at 55°C for 30 s, an extension
320 at 72°C for 90 s, and a final extension at 72°C for 5 mins. We ran the PCR products on a 1%
321 agarose gel and visualized them under ultraviolet light after staining with SYBR Safe
322 (Invitrogen) to confirm the absence of bacteria in axenic individuals and the presence of
323 bacteria in controls.

324 We maintained all females and standard competitors as axenic flies throughout the
325 experiment and supplemented axenic focal males with different bacterial cultures to produce
326 gnotobiotic associations as described below. All adult food was free of antibiotics.
327
328 **Bacterial cultures and gnotobiotic associations**
329 Throughout this study, we used five bacterial species isolated from the gut of wild-type flies
330 (17): *Acetobacter orientalis*, *A. tropicalis*, *A. pasteurianus*, *Lactobacillus plantarum*, and *L.*
331 *brevis*. We associated our focal flies with all 32 possible combinations among these bacterial
332 strains following the general protocol of Gould et al. (17). To prepare bacterial cultures, we
333 grew them overnight: *Lactobacillus* spp. in MRS (De Man–Rogosa–Sharpe) broth without
334 shaking and *Acetobacter* spp. in MRS + mannitol medium at 30°C on a shaker. The next
335 morning, we checked these bacterial cultures for growth and performed their optical density
336 (OD) measurements at 600 nm. Then, we spun down these different bacterial cultures at 7000
337 rpm for 5 minutes and resuspended the resulting pellets to a concentration of 10^8 cells/mL in
338 sterile phosphate-buffered saline (PBS). Resuspension volume was determined following
339 established protocols (50, 51). Finally, we added a 50 µl (i.e., ca. 5×10^6 colony forming units,
340 CFUs) of bacterial culture to sterile (but antibiotic-free) fly food vials, adjusting the volume
341 per bacterial strain in multi-species associations for equal representation within a consistent
342 total density, which itself was comparable to prior reports for conventional flies (17, 51).
343 After adding the bacteria to food vials and air-drying these under in laminar flow hood,
344 we transferred 10 one-day-old axenic virgin males to each vial for inoculation with the added
345 bacterial strains. We moved these males to fresh food vials with same bacterial treatment every
346 alternate day for 5 days. Thereafter, we confirmed gnotobiotic associations by plating together
347 the homogenates of 3-4 adult flies from same treatments and checking their colony
348 morphologies, and by Sanger sequencing of 16S PCR homogenates. For multi-associations, we

349 plated the fly homogenates and picked the distinct types of colonies from a given plate for PCR
350 and performed sequencing to confirm that morphologically similar species corresponds to same
351 species in all the replicates, thus allowing us to distinguish between different bacterial species
352 by looking at their colony appearance. Thereafter, we tested the presence of the expected
353 bacterial species in a particular bacterial combination by plating them and looking at the colony
354 morphologies.
355
356 **Bacterial abundance in different combinations**
357 To determine bacterial abundance in different gnotobiotic associations, we counted the CFUs
358 per fly for each bacterial species across the different gnotobiotic associations. To this end, we
359 washed males with 70% ethanol, individually homogenized them with a pestle in
360 microcentrifuge tubes, and then diluted these homogenates to different dilutions with a final
361 volume of 100 µl to find a dilution with comparable colony counts (approx. 100 CFUs) for
362 visual quantification. In gnotobiotic cultures with both bacterial genera, we transferred an
363 aliquot of well-mixed fly homogenate to two plates, supplementing the MRS media of one
364 plate with 10 µg/ml ampicillin to selectively inhibit the growth of *Lactobacillus*, while
365 incubating the other in a CO_2 atmosphere to prevent the growth of *Acetobacter*. We achieved
366 within-genus differentiation of strains by colony morphologies: *A. orientalis* with flat colonies
367 with ruffled borders, *A. tropicalis* with small tan coloured and highly reflective colonies, and
368 *A. pasteurianus* with large tan colonies. Similarly, *L. brevis* produces brownish yellow colonies
369 and *L. plantarum* milky white colonies (Supplementary Fig. S8). Using 16S PCR amplification
370 followed by Sanger sequencing, we confirmed specificity of these colony properties,
371 demonstrating the robustness of our method based on morphological identifications during
372 experiments. After counting the number of colonies on each plate, we calculated CFU per fly

373 as CFU = $C \times D \times V / P$, where C = number of colonies counted, D = dilution factor, V =
374 volume of fly homogenate, and P = volume plated (50).
375 Across all 10 replicate plates combination examined, the expected species were present,
376 and none of the remaining species. Consistent with Gould et al. (17), total CFU counts
377 increased with species richness while the species-specific abundances declined
378 (Supplementary Fig. S9).
379
380 **Sperm competitive ability**
381 To investigate sperm competitiveness of focal males, we quantified their sperm offense ability
382 (P_2) by mating them as the second males with axenic females that had each mated with a an
383 axenic GFP male three days earlier. We monitored the occurrence of copulations for 7-8 hours
384 and transferred remated females to oviposition vials while giving those that did not remate
385 another two 8-hour remating opportunities on the following days. Flies that did not remate by
386 the last opportunity (within these 3 days) were discarded. We allowed all remated females to
387 lay eggs for three days. After all progeny eclosed, we scored them for paternity under a
388 fluorescence stereoscope, based on the presence/absence of the ubiquitous GFP marker in
389 standard competitors. The proportion of second-male progeny indicated the focal-male sperm
390 competitive ability (i.e., sperm offense). We replicated this experiment thrice with 30 replicates
391 per bacterial treatment each time (total N = 2,880 trials).
392
393 **Sperm viability**
394 We quantified sperm viability for 10 males per bacterial treatment (total N = 320 males). Once
395 males were six days old and inoculated, we anaesthetized them on ice and dissected them on a
396 microscopic slide to isolate the seminal vesicles from their reproductive tissue. We then placed
397 one of the seminal vesicles in 10 μl of Ringers solution and punctured it with an insect pin to

398 release the sperm mass for immediate staining with LIVE/DEAD fluorescent dye, following
399 the principles of prior studies on *Drosophila* (31, 52). This two-component dye consists of
400 SYBR-14 ('LIVE' component emitting green fluorescence), which is actively incorporated
401 into living cells, and propidium iodide (PI, with red fluorescence) that can only permeate
402 damaged membranes (typical of dead cells). We prepared an aqueous staining solution by
403 combining 2.4 µl of SYBR-14 stock solution (1 mM in DMSO) and 4.5 µl of PI stock solution
404 (2.4 mM in water) in 93.1 µl of Ringer's solution. Then, we added 5 µl of the staining solution
405 to the sperm sample before covering it with a coverslip and incubating it for 5 minutes in the
406 dark. Under an Olympus BX50 fluorescence microscope with a GFP/RFP dual filter, we
407 captured images of randomly chosen areas of each sample to later manually count at least 200
408 sperm and calculate the proportion of viable sperm in ImageJ v. 1.34(53).
409
410 **Visualizing sperm competition within female reproductive tract**
411 Since competitive fertilization events ultimately are the result of both male and female effects
412 (42, 54), we investigated how females bias their sperm storage based on interactions with males
413 supplemented with different microbiome. For this experiment, we again mated axenic virgin
414 females first with an axenic GFP male and, three days later, with a focal male as for sperm
415 competitive ability (above). To visualize sperm of both males, we used focal males expressing
416 RFP in their sperm heads. Immediately after remating, we transferred females to individual
417 wells of cell-culture plates, with a coverslip held in place with dots of rubber cement in two
418 corners. We checked these females every 10 min for up to 6 h for the ejection of the sperm
419 mass containing both displaced first-male and excess second-male sperm (32, 43). The timing
420 and extent of sperm ejection have previously been reported to affect relative numbers of first-
421 and second-male sperm stored by females and, consequently, competitive fertilization success
422 among males (33, 42).

423 Upon female sperm ejection, we recorded the interval from mating to ejection before
424 removing females from the well and freezing them individually in Eppendorf tubes. Thereafter,
425 we dissected these females and counted the green (standard competitors) and red sperm (focal
426 males) within the female reproductive tract (paired spermathecae, seminal receptacle and bursa
427 copulatrix) under a fluorescence microscope. From these counts, we determined S_2, the
428 proportion of all sperm stored by the female that came from the second (experimental) male.
429 We also counted the respective sperm numbers in the ejected sperm mass to estimate, combined
430 with above counts, the total number of sperm transferred by the second male and the number
431 of first-male sperm still residing in storage at the time of remating. This experiment was
432 performed in five blocks with 10 replicates per treatment for each block (total N = 1,600
433 remating trials).
434
435 **Statistical analyses**
436 All analyses were conducted in R v4.4.3 (R Core Team 2025), using bootstrapping procedures
437 with 1,000 iterations to assess the stability and robustness of model estimates. To evaluate the
438 effects of microbial diversity on reproductive outcomes, we resampled microbiome
439 compositions (N = 32 unique consortia) and fitted mixed-effects models across all bootstrap
440 datasets. These models included species richness (number of bacterial species) as a fixed effect
441 and both experimental block and microbial composition (i.e., consortium identity) as random
442 effects. Depending on the response variable, models were either linear mixed-effects models
443 (for traits such as the number of sperm transferred and time to sperm ejection) or generalized
444 linear mixed-effects models with a binomial error distribution and logit link function (for
445 proportions of viable sperm, second-male sperm in storage, and second-male progeny).
446 Binomial models included an observation-level random effect to account for overdispersion.

447 To examine the contribution of specific microbial interactions, we fitted similar mixed-
448 effects models using the presence/absence of each bacterial species and their two- to five-way
449 interactions as fixed effects, with block and, where appropriate, observation identity as random
450 effects. In this interaction-focused analysis, we bootstrapped at the level of individual
451 observations, stratified by microbial consortium, to retain the structure of specific
452 combinations. All subsequent analyses used the same set of bootstrapped datasets for
453 consistency and comparability.

454 To better understand the importance of species combinations in the microbiome and to
455 isolate emergent effects beyond individual species contributions, we used an epistasis-based
456 framework to elucidate how well the averaged phenotypic effects of single- or pairwise species
457 associations predict higher-order phenotypes (17). For single-species predictions, we compared
458 the measured trait values of males associated with two- to five-species microbiotas to values
459 averaged across mono-associated males that jointly represented the same bacterial
460 combinations. These differences (averaged prediction minus measured trait value) were then
461 plotted with bootstrapped 95% confidence intervals to visually determine if predictions
462 deviated from the measured estimates (i.e., confidence interval excluding zero difference). We
463 then repeated this procedure to predict phenotypes by averaging the estimates of di-associated
464 males (for calculations see (17)).

465 Following the same general principle, we further quantified how the presence or absence
466 of non-focal ("bystander") community members modulates both pairwise and three-way
467 microbial interactions by exhaustively enumerating all possible bystander contexts. We then
468 compared this "contextual" analysis against a "standard" test to reveal how higher-order
469 community background shapes emergent effects on host traits. Following Gould et al.'s (17)
470 nomenclature, the "standard" test calculated the interaction coefficient among all species
471 present in a specific community configuration, whereas the "contextual" tests assessed the

interaction between a focal species pair within the context of additional bystander species. We computed interaction coefficients for each focal species pair or triplet across all possible presence/absence combinations of bystander species and plotted them with bootstrapped standard errors to highlight the varying directions of interactions depending on the bystander combinations.

In both the single/double-species predictions and these standard/contextual tests, we derived the coefficients to calculate the deviations from a mixed-effects models with an appropriate link function for each microbial combination, controlling for block effects. We repeated each model across 1,000 bootstrapped datasets to calculate the standard errors or 95% confidence intervals from the distribution of the calculated coefficient or interaction differentials.

Acknowledgements

We thank W. Ludington for providing the five bacterial strains used in our experiments.

Funding

This project was supported by the Swiss National Science Foundation (grant PP00P3_202662 to S.L.).

Author contributions

K.M.: conceptualization, methodology, investigation, data collection and curation, data analysis, writing original draft, writing—review and editing, project administration; A.M.: investigation, data collection, writing—review and editing; A.N.D.N: investigation, data collection, writing—review and editing; S.H.S: investigation, writing—review and editing; J.R.: investigation; S.L.: conceptualization, methodology, funding acquisition, data analysis,

project administration, supervision, writing original draft, writing manuscript—review and editing.

All authors gave final approval for publication and have agreed to be held accountable for the work performed therein.

Competing interests

All authors declare that they have no conflict of interest.

REFERENCES

1. L. W. Simmons, J. L. Fitzpatrick, Sperm wars and the evolution of male fertility. *Reproduction* **144**, 519–534 (2012).
2. J. L. Fitzpatrick, S. Lüpold, Sexual selection and the evolution of sperm quality. *Mol. Hum. Reprod.* **20**, 1180–1189 (2014).
3. D. A. Dewsbury, Ejaculate cost and male choice. *Am. Nat.* **119**, 601–610 (1982).
4. S. Lüpold, *et al.*, How sexual selection can drive the evolution of costly sperm ornamentation. *Nature* **533**, 535–538 (2016).
5. M. Olsson, T. Madsen, R. Shine, Is sperm really so cheap? Costs of reproduction in male adders, *Vipera berus*. *Proc. R. Soc. B* **264**, 455–459 (1997).
6. J. C. Perry, C. T. Tse, Extreme costs of mating for male two-spot ladybird beetles. *PLoS ONE* **8**, e81934 (2013).
7. E. L. Macartney, A. J. Crean, S. Nakagawa, R. Bonduriansky, Effects of nutrient limitation on sperm and seminal fluid: a systematic review and meta-analysis. *Biol. Rev.* **94**, 1722–1739 (2019).

8. Y. Iwasa, A. Pomiankowski, S. Nee, The evolution of costly mate preferences. II. The handicap principle. *Evolution* **45**, 1431–1442 (1991).

9. A. Grafen, Sexual selection unhandicapped by the Fisher process. *J. Theor. Biol.* **144**, 517–546 (1990).

10. L. Rowe, D. Houle, The lek paradox and the capture of genetic variance by condition dependent traits. *Proc. R. Soc. B* **263**, 1415–1421 (1996).

11. G. E. Hill, Condition-dependent traits as signals of the functionality of vital cellular processes. *Ecol. Lett.* **14**, 625–634 (2011).

12. E. C. Lindsay, N. B. Metcalfe, M. S. Llewellyn, The potential role of the gut microbiota in shaping host energetics and metabolic rate. *J. Anim. Ecol.* **89**, 2415–2426 (2020).

13. T. O. Cox, P. Lundgren, K. Nath, C. A. Thaiss, Metabolic control by the microbiome. *Genome Med.* **14**, 80 (2022).

14. A. E. Douglas, The microbial dimension in insect nutritional ecology. *Funct. Ecol.* **23**, 38–47 (2009).

15. J. Alcock, C. C. Maley, C. A. Aktipis, Is eating behavior manipulated by the gastrointestinal microbiota? Evolutionary pressures and potential mechanisms. *BioEssays* **36**, 940–949 (2014).

16. S. O. Fetissov, Role of the gut microbiota in host appetite control: bacterial growth to animal feeding behaviour. *Nat. Rev. Endocrinol.* **13**, 11–25 (2017).

17. A. L. Gould, *et al.*, Microbiome interactions shape host fitness. *Proc. Natl. Acad. Sci. U. S. A.* **115**, E11951–E11960 (2018).

18. A. W. Walters, *et al.*, The microbiota influences the *Drosophila melanogaster* life history strategy. *Mol. Ecol.* **29**, 639–653 (2020).

19. V. Emelianoff, *et al.*, A survival-reproduction trade-off in entomopathogenic nematodes mediated by their bacterial symbionts. *Evolution* **62**, 932–942 (2008).

546 20. X. Qi, C. Yun, Y. Pang, J. Qiao, The impact of the gut microbiota on the reproductive
547 and metabolic endocrine system. *Gut Microbes* **13**, 1894070 (2021).
548 21. P. Comizzoli, M. L. Power, S. L. Bornbusch, C. R. Muletz-Wolz, Interactions between
549 reproductive biology and microbiomes in wild animal species. *Anim. Microbiome* **3**, 87
550 (2021).
551 22. S. B. Chadchan, V. Singh, R. Kommagani, Female reproductive dysfunctions and the gut
552 microbiota. *J. Mol. Endocrinol.* **69**, R81–R94 (2022).
553 23. M. K. Matthews, J. Malcolm, J. M. Chaston, Microbiota influences fitness and timing of
554 reproduction in the fruit fly *Drosophila melanogaster*. *Microbiol. Spectr.* **9**, e0003421
555 (2021).
556 24. M. Al-Asmakh, *et al.*, The gut microbiota and developmental programming of the testis
557 in mice. *PLoS ONE* **9**, e103809 (2014).
558 25. N. Ding, *et al.*, Impairment of spermatogenesis and sperm motility by the high-fat diet-
559 induced dysbiosis of gut microbes. *Gut* **69**, 1608–1619 (2020).
560 26. M. Alfano, *et al.*, Testicular microbiome in azoospermic men—first evidence of the
561 impact of an altered microenvironment. *Hum. Reprod.* **33**, 1212–1217 (2018).
562 27. S.-L. Weng, *et al.*, Bacterial communities in semen from men of infertile couples:
563 metagenomic sequencing reveals relationships of seminal microbiota to semen quality.
564 *PloS One* **9**, e110152 (2014).
565 28. E. V. Ridley, A. C. N. Wong, A. E. Douglas, Microbe-dependent and nonspecific effects
566 of procedures to eliminate the resident microbiota from *Drosophila melanogaster*. *Appl.*
567 *Environ. Microbiol.* **79**, 3209–3214 (2013).
568 29. A. C.-N. Wong, J. M. Chaston, A. E. Douglas, The inconstant gut microbiota of
569 *Drosophila* species revealed by 16S rRNA gene analysis. *ISME J.* **7**, 1922–1932 (2013).

570 30. J. G. McMullen, G. Peters-Schulze, J. Cai, A. D. Patterson, A. E. Douglas, How gut
571 microbiome interactions affect nutritional traits of *Drosophila melanogaster*. *J. Exp.*
572 *Biol.* **223** (2020).
573 31. M. Tourmente, C. R. Archer, D. J. Hosken, Complex interactions between sperm viability
574 and female fertility. *Sci. Rep.* **9**, 15366 (2019).
575 32. S. Lüpold, *et al.*, How multivariate ejaculate traits determine competitive fertilization
576 success in *Drosophila melanogaster*. *Curr. Biol.* **22**, 1667–1672 (2012).
577 33. S. Lüpold, *et al.*, Female mediation of competitive fertilization success in *Drosophila*
578 *melanogaster*. *Proc. Natl. Acad. Sci. U. S. A.* **110**, 10693–10698 (2013).
579 34. A. C.-N. Wong, A. J. Dobson, A. E. Douglas, Gut microbiota dictates the metabolic
580 response of *Drosophila* to diet. *J. Exp. Biol.* **217**, 1894–1901 (2014).
581 35. C. C. Maresch, *et al.*, Diabetes-induced hyperglycemia impairs male reproductive
582 function: a systematic review. *Hum. Reprod. Update* **24**, 86–105 (2018).
583 36. S. Subhadarshini, V. Mallesh, G. K. Bharath, Semen quality alterations in men with
584 hyperlipidemia and diabetes mellitus: a cross-sectional study. *Int. J. Acad. Med. Pharm.*
585 **6**, 639–644 (2024).
586 37. S. C. Shin, *et al.*, *Drosophila* microbiome modulates host developmental and metabolic
587 homeostasis via insulin signaling. *Science* **334**, 670–674 (2011).
588 38. I. Iatsenko, J.-P. Boquete, B. Lemaitre, Microbiota-derived lactate activates production of
589 reactive oxygen species by the intestinal NADPH oxidase nox and shortens *Drosophila*
590 lifespan. *Immunity* **49**, 929-942.e5 (2018).
591 39. R. J. Aitken, Z. Gibb, M. A. Baker, J. Drevet, P. Gharagozloo, Causes and consequences
592 of oxidative stress in spermatozoa. *Reprod. Fertil. Dev.* **28**, 1–10 (2016).
593 40. A. Zelezniak, *et al.*, Metabolic dependencies drive species co-occurrence in diverse
594 microbial communities. *Proc. Natl. Acad. Sci.* **112**, 6449–6454 (2015).

41. L. Rowe, D. Houle, The lek paradox and the capture of genetic variance by condition dependent traits. *Proc. R. Soc. Lond. B Biol. Sci.* **263**, 1415–1421 (1996).

42. S. Lüpold, *et al.*, How female × male and male × male interactions influence competitive fertilization in *Drosophila melanogaster*. *Evol. Lett.* **4**, 416–429 (2020).

43. M. K. Manier, *et al.*, Resolving mechanisms of competitive fertilization success in *Drosophila melanogaster*. *Science* **328**, 354–357 (2010).

44. L. P. Henry, M. Bruijning, S. K. Forsberg, J. F. Ayroles, The microbiome extends host evolutionary potential. *Nat. Commun.* **12**, 5141 (2021).

45. N. A. Moran, H. Ochman, T. J. Hammer, Evolutionary and ecological consequences of gut microbial communities. *Annu. Rev. Ecol. Evol. Syst.* **50**, 451–475 (2019).

46. R. C. Firman, C. Gasparini, M. K. Manier, T. Pizzari, Postmating female control: 20 years of cryptic female choice. *Trends Ecol. Evol.* **32**, 368–382 (2017).

47. L. Daupagne, *et al.*, One size does not fit all: female–male interactions on the path to fertilization. (2025). https://doi.org/10.1530/REP-24-0238.

48. E. L. Macartney, *et al.*, Sperm depletion in relation to developmental nutrition and genotype in *Drosophila melanogaster*. *Evolution* **75**, 2830–2841 (2021).

49. V. Zeender, S. Pfammatter, B. Roschitzki, S. Dorus, S. Lüpold, Genotype-by-environment interactions influence the composition of the *Drosophila* seminal proteome. *Proc. R. Soc. B* **290**, 20231313 (2023).

50. M. L. Koyle, *et al.*, Rearing the fruit fly *Drosophila melanogaster* under axenic and gnotobiotic conditions. *J. Vis. Exp.* **113**, e54219 (2016).

51. P. D. Newell, A. E. Douglas, Interspecies interactions determine the impact of the gut microbiota on nutrient allocation in *Drosophila melanogaster*. *Appl. Environ. Microbiol.* **80**, 788–796 (2014).

52. A. Meena, *et al.*, Fertility loss and recovery dynamics after repeated heat stress across life stages in male *Drosophila melanogaster*: Patterns and processes. *R. Soc. Open Sci.* **11**, 241082 (2024).

53. C. A. Schneider, W. S. Rasband, K. W. Eliceiri, NIH Image to ImageJ: 25 years of image analysis. *Nat. Methods* **9**, 671–675 (2012).

54. W. G. Eberhard, *Female Control: Sexual Selection by Cryptic Female Choice* (Princeton University Press, 1996).

627 **Figures**

628 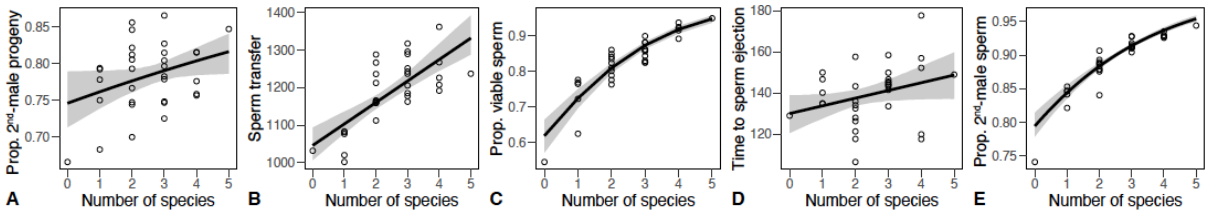

629 **Fig. 1.** Associations between the number of bacterial species in the microbiota and the different
630 fitness traits. Each point indicates the mean of all replicate samples for a given microbiome
631 consortium (N = 32). The lines and 95% confidence bands are derived from bootstrapped
632 (generalized) linear mixed-effects models with microbiome composition and experimental
633 block as random effects (for binomial models additionally also an observation-level random
634 effect).

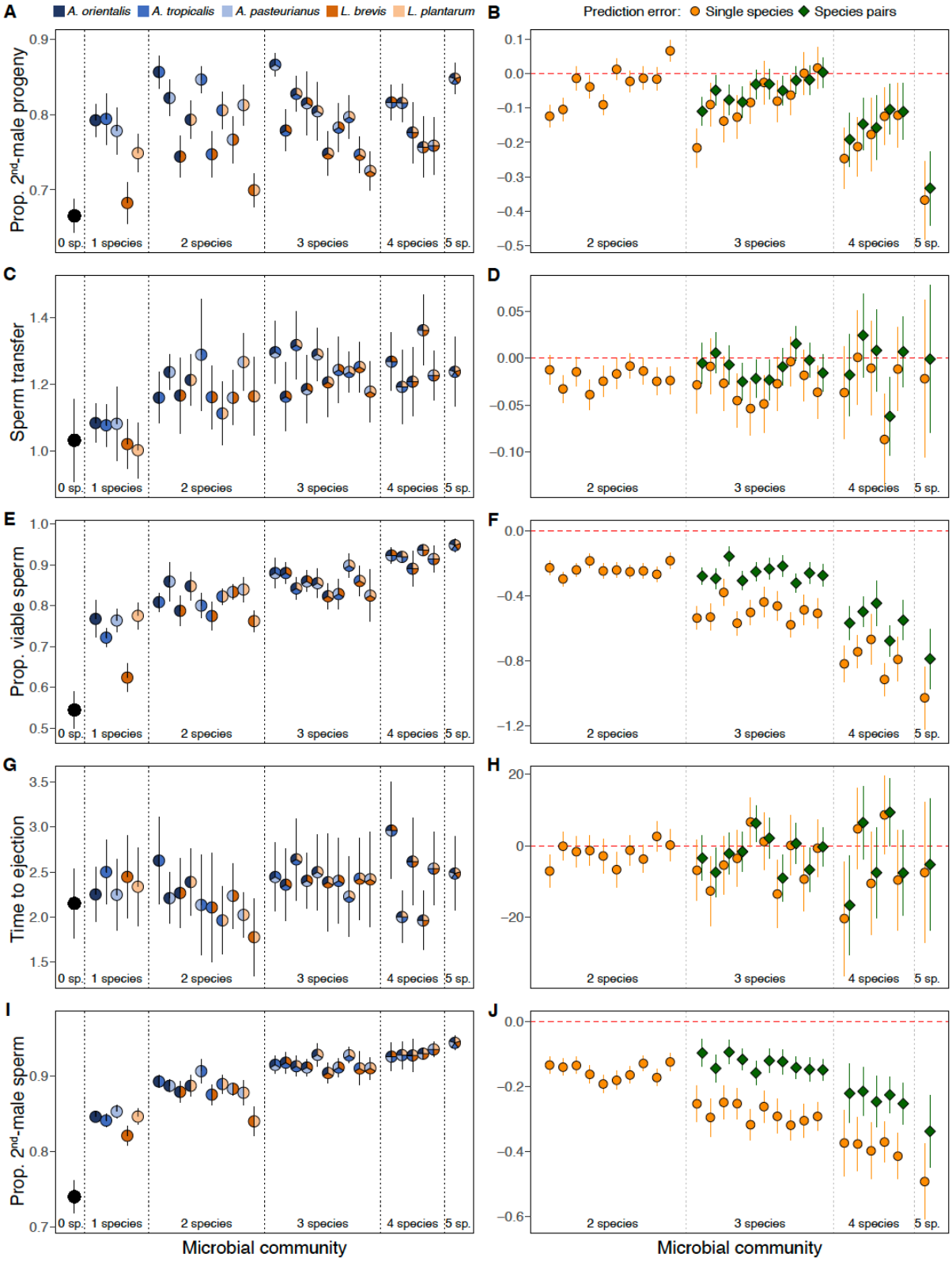

Fig. 2. Variation in male fitness traits relative to their microbial community (left) and error in predicting these values for males associated with multiple species based on single- or pairwise species averages (right). In the left panels, colours indicate the different combinations of

Acetobacter and *Lactobacillus* species associated with experimental males. The right panels depict the deviations in trait predictions from measured traits by averaging the corresponding coefficients of (generalized) linear mixed-effects models for individual species (orange points) or species pairs (green diamonds) that jointly represented the same species communities. The relevant microbial combinations are plotted in the same order across all panels. Error bars reflect 95% confidence intervals (from raw distributions in left panels, from bootstrapped prediction differentials in right panels). Sperm transfer in thousands, time to sperm ejection in hours, other variables in proportions.

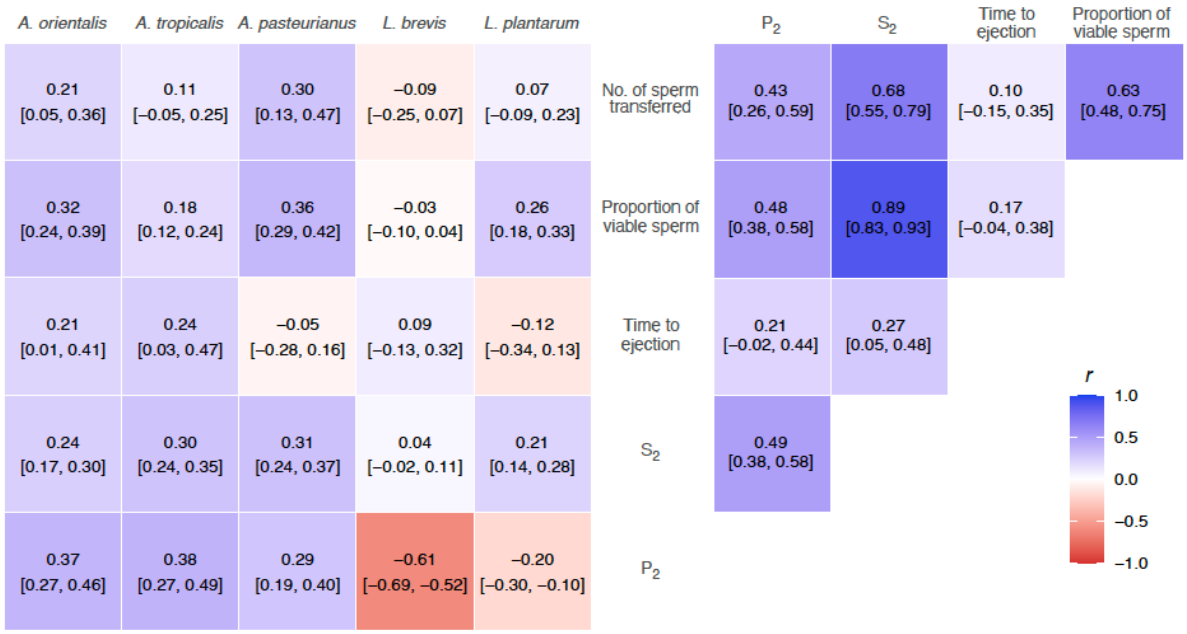

Fig. 3. Correlations between the different phenotypic traits and the relative abundance (based on CFU counts) of each of the five bacterial species (left) and among the traits themselves (right). Values reflect the averaged correlation coefficients with 95% confidence limits of pairwise Pearson correlations across bootstrapped group means (N = 1,000 samples) among males with a given microbiome consortium. Relative abundances and proportional traits (sperm viability, S_2, P_2) were logit-transformed before bootstrapping. Colours indicate the strength and direction of correlations as reflected by the colour-gradient bar.

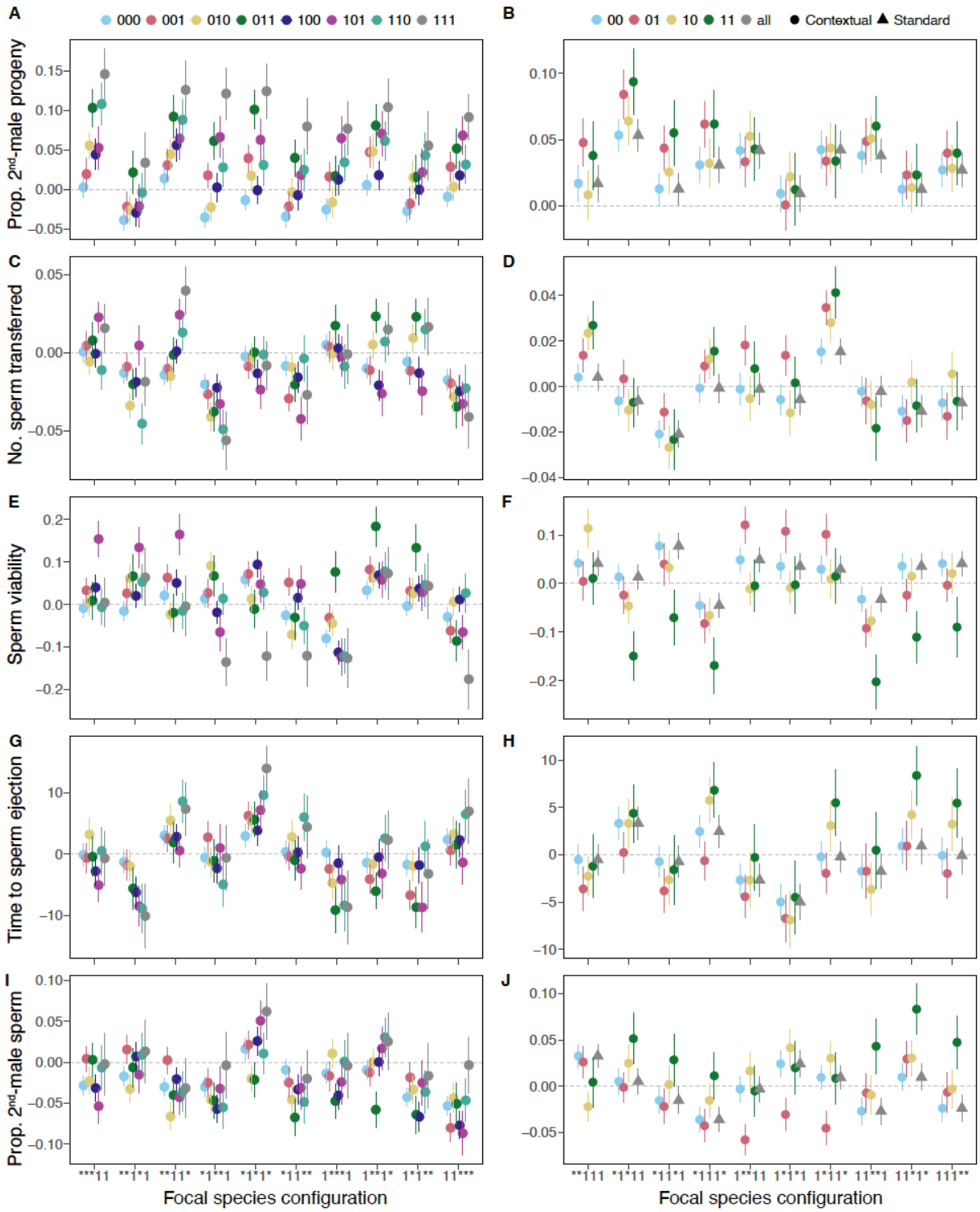

Fig. 4. Interactive effects between bacterial species contingent on bystander species, with two-way interactions between pairs of focal of species in the left panels, and three-way interactions between trios of focal species in the right panels. For each code along the x-axes, 1's indicate the species configuration of the interaction and asterisks denote placeholders for bystander

species (order within codes from left to right: *A. orientalis*, *A. tropicalis*, *A. pasteurianus*, *L. brevis*, *L. plantarum*). The binary codes in the legends indicate the configuration of bystanders in the order, in which they would fill the placeholders (*) in each focal species configuration (1 = presence, 0 = absence). The right panels distinguish between the “standard” tests (grey triangles; i.e., global interaction across all community members present) and "contextual" tests (coloured points; i.e., separate interactions between a focal species pair or triplet for each bystander combination) for each focal triplet. All coefficients and propagated standard errors were derived from (generalized) linear mixed-effects models across 1,000 bootstrapped datasets.

670 **Supplementary figures**
671

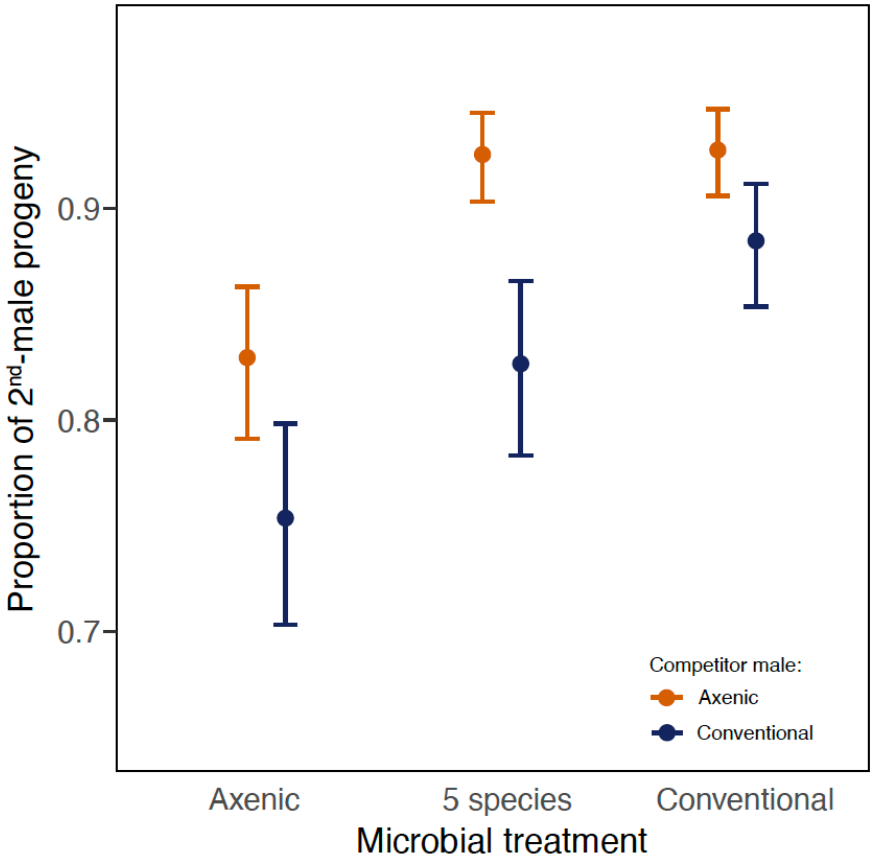

672
673
674 **Supplementary Figure S1:** Competitive fertilization success, measured as the proportion of second-
675 male (i.e., focal-male) paternity, against either axenic or conventional competitors (first males to mate).
676 In either context, males that were associated with the five-species microbial consortium (*Acetobacter*
677 *orientalis*, *A. tropicalis*, *A. pasteurianus*, *Lactobacillus brevis* and *L. plantarum*) after axenic
678 development outperformed consistently germ-free (axenic) males and even matched males with a
679 conventional (entirely unmanipulated) microbiome in their sperm competitiveness, at least against
680 germ-free competitors. Error bars represent 95% confidence intervals.
681

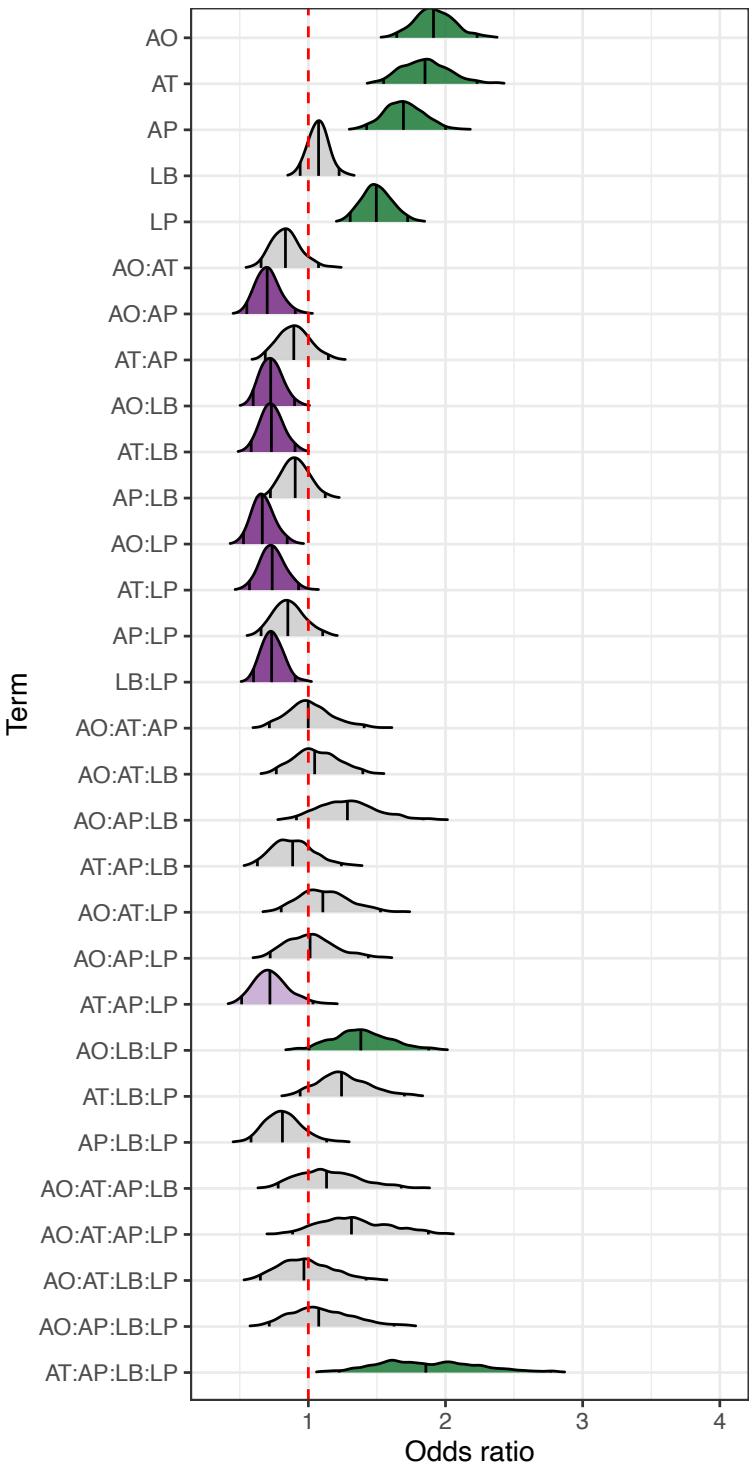

Supplementary Figure S2: Ridge plot showing the distribution of fixed-effect odds ratios across 1,000 bootstrap iterations of a generalized linear mixed-effects model on the proportion of focal-male progeny in sperm competition against axenic males. The model includes all main effects and two- to four-way interactions among five bacterial species. Each ridge represents the distribution of bootstrapped estimates for a given term, and its stability. Ridge colours indicate the direction of the effect (green: positive; purple: negative), with darker shades denoting effects whose 95% confidence intervals exclude zero, and lighter shades for those where only the 90% confidence interval excludes zero. The vertical dashed line indicates no effect.

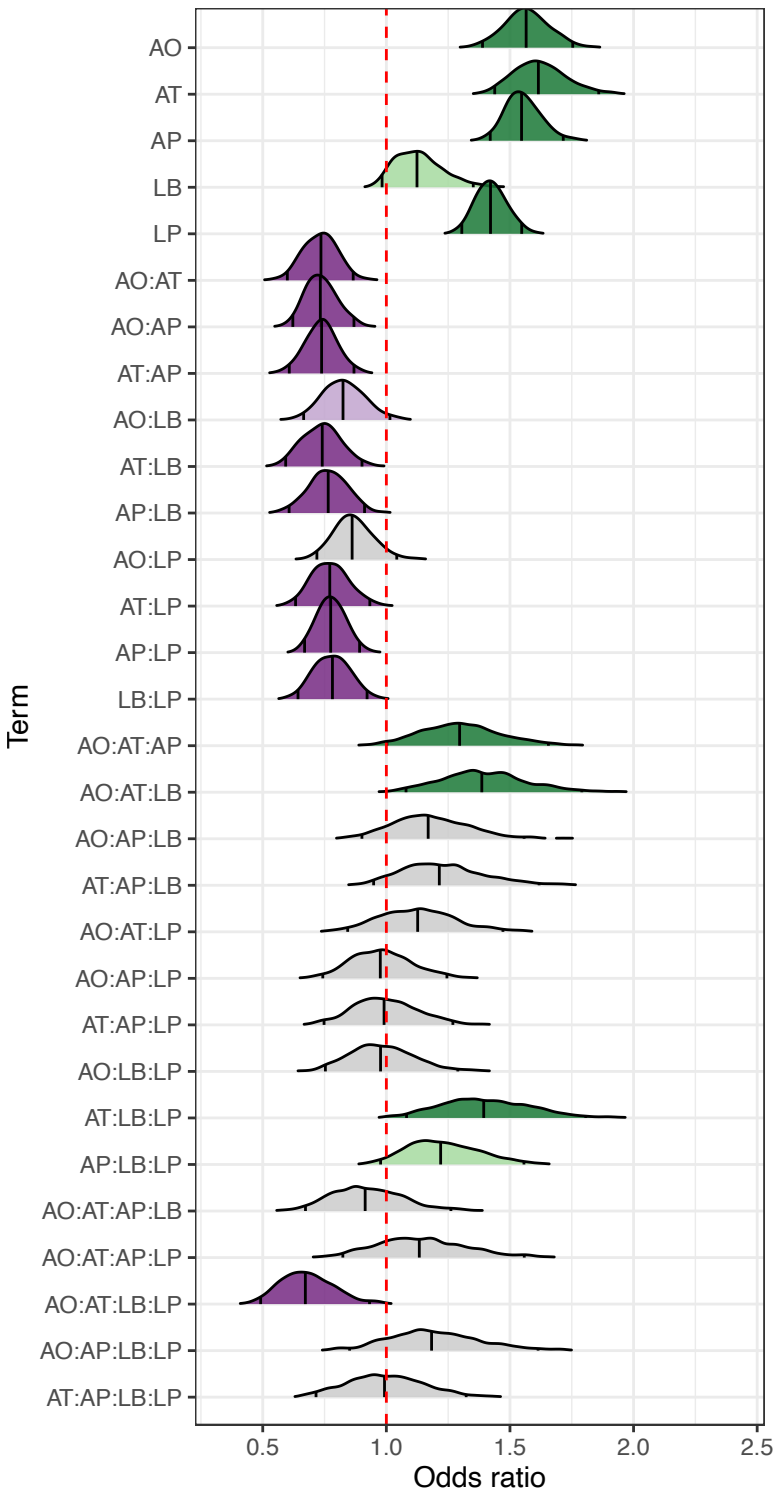

Supplementary Figure S3: Ridge plot showing the distribution of fixed-effect odds ratios across 1,000 bootstrap iterations of a generalized linear mixed-effects model on the proportion of focal-male progeny in sperm competition against males with an intact microbiome. The model includes all main effects and two- to four-way interactions among five bacterial species. Each ridge represents the distribution of bootstrapped estimates for a given term, and its stability. Ridge colours indicate the direction of the effect (green: positive; purple: negative), with darker shades denoting effects whose 95% confidence intervals exclude zero, and lighter shades for those where only the 90% confidence interval excludes zero. The vertical dashed line indicates no effect.

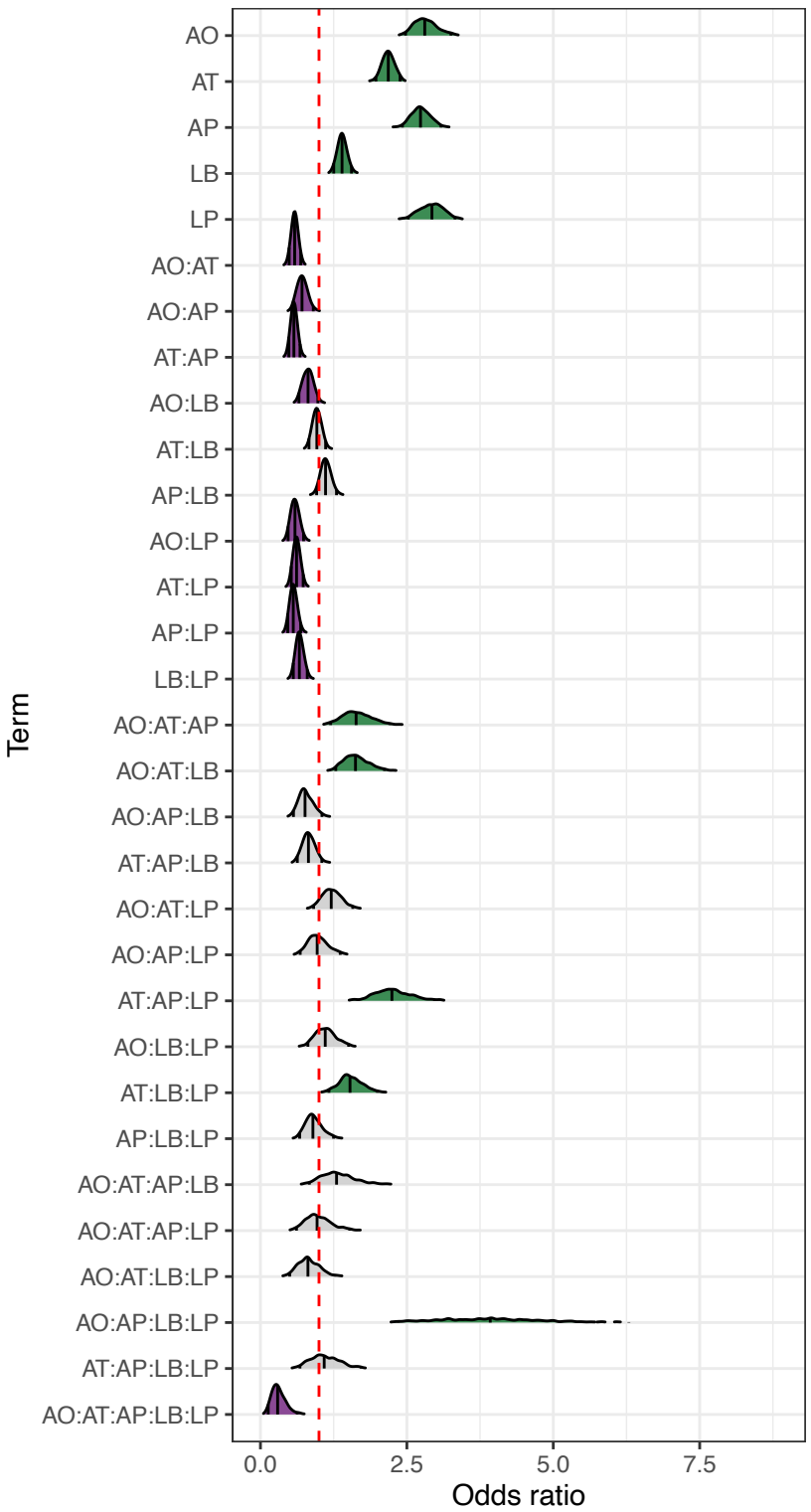

Supplementary Figure S4: Ridge plot showing the distribution of fixed-effect odds ratios across 1,000 bootstrap iterations of a generalized linear mixed-effects model on the proportion of viable sperm. The model includes all main effects and two- to four-way interactions among five bacterial species. Each ridge represents the distribution of bootstrapped estimates for a given term, and its stability. Ridge colours indicate the direction of the effect (green: positive; purple: negative) where 95% confidence intervals exclude zero. The vertical dashed line indicates no effect.

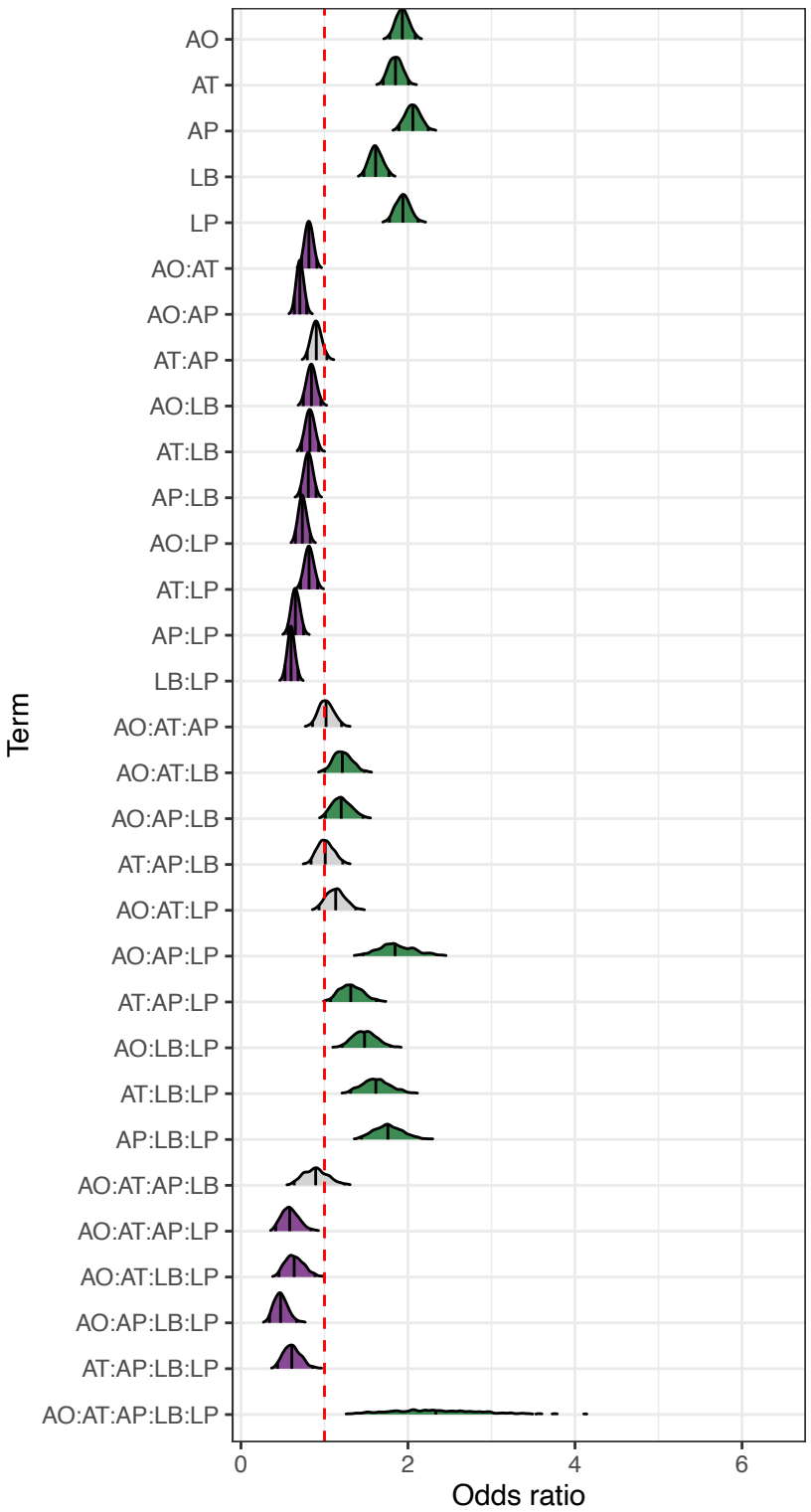

Supplementary Figure S5: Ridge plot showing the distribution of fixed-effect odds ratios across 1,000 bootstrap iterations of a generalized linear mixed-effects model on the proportion of focal-male sperm remaining in female storage after sperm ejection. The model includes all main effects and two- to four-way interactions among five bacterial species. Each ridge represents the distribution of bootstrapped estimates for a given term, and its stability. Ridge colours indicate the direction of the effect (green: positive; purple: negative) where 95% confidence intervals exclude zero. The vertical dashed line indicates no effect.

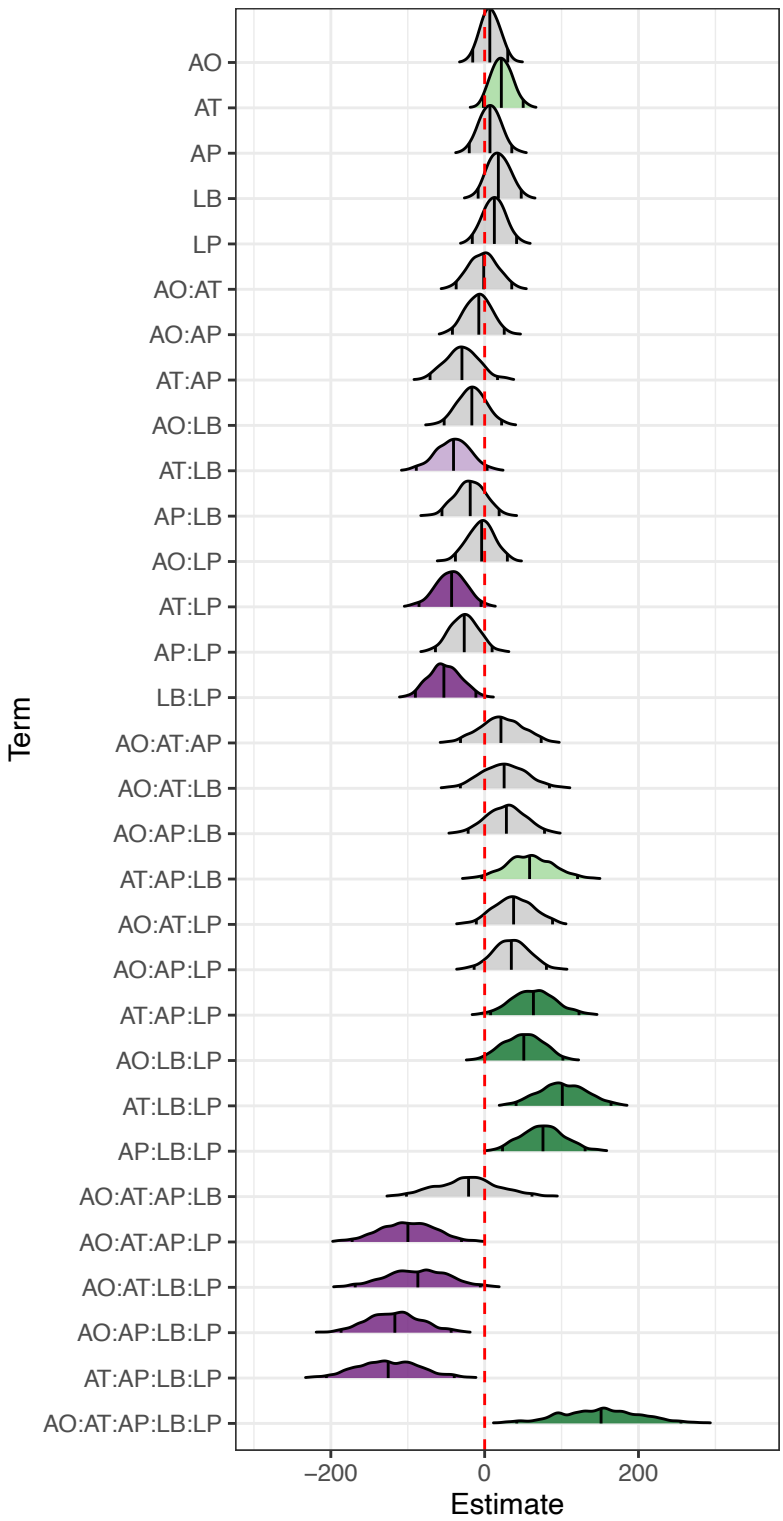

Supplementary Figure S6: Ridge plot showing the distribution of fixed-effect estimates across 1,000 bootstrap iterations of a linear mixed-effects model on the time to female sperm ejection. The model includes all main effects and two- to four-way interactions among five bacterial species. Each ridge represents the distribution of bootstrapped estimates for a given term, and its stability. Ridge colours indicate the direction of the effect (green: positive; purple: negative), with darker shades denoting effects whose 95% confidence intervals exclude zero, and lighter shades for those where only the 90% confidence interval excludes zero. The vertical dashed line indicates no effect. Estimates in minutes.

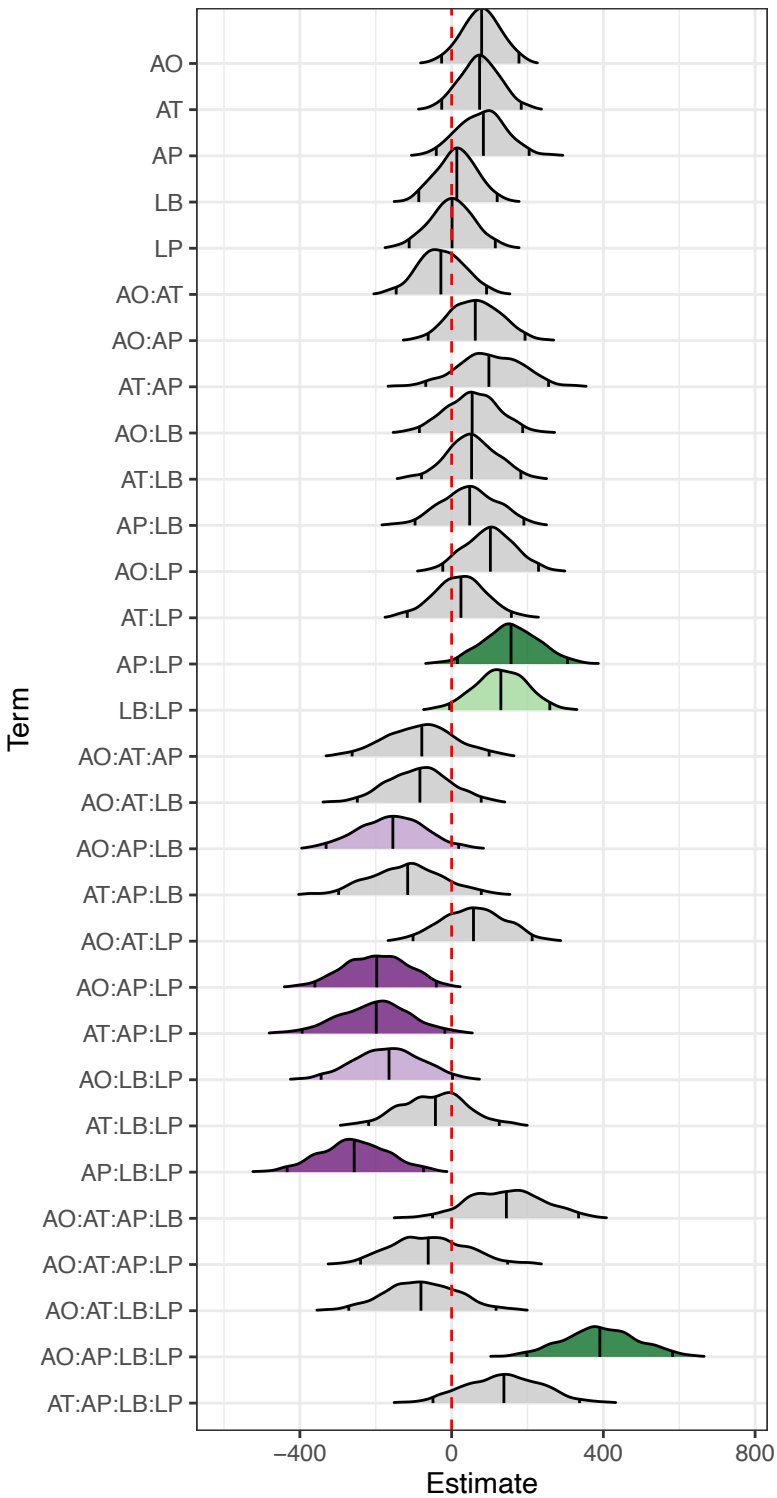

Supplementary Figure S7: Ridge plot showing the distribution of fixed-effect estimates across 1,000 bootstrap iterations of a linear mixed-effects model on the number of sperm transferred by focal males. The model includes all main effects and two- to four-way interactions among five bacterial species. Each ridge represents the distribution of bootstrapped estimates for a given term, and its stability. Ridge colours indicate the direction of the effect (green: positive; purple: negative), with darker shades denoting effects whose 95% confidence intervals exclude zero, and lighter shades for those where only the 90% confidence interval excludes zero. The vertical dashed line indicates no effect. Estimates in raw sperm counts.

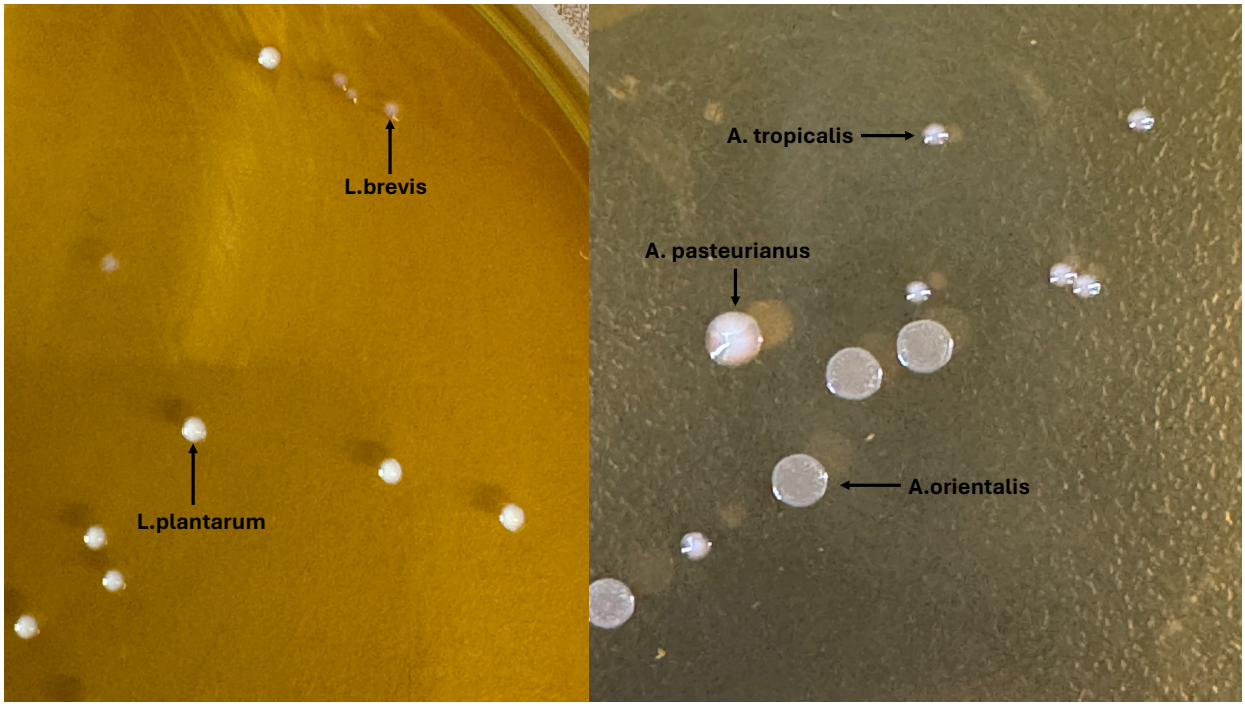

Supplementary Figure S8: Image showing morphological appearances of colonies formed by different bacterial species. On right side, acetobacter strains are present with *Acetobacter orientalis* represented by flat colonies with ruffled borders, *Acetobacter tropicalis* with small tan colored and highly reflective colonies, and *Acetobacter pasteurianus* with large tan colonies. In contrast on left side, *Lactobacillus brevis* shows brownish yellow colonies and *Lactobacillus plantarum* with milky white colonies.

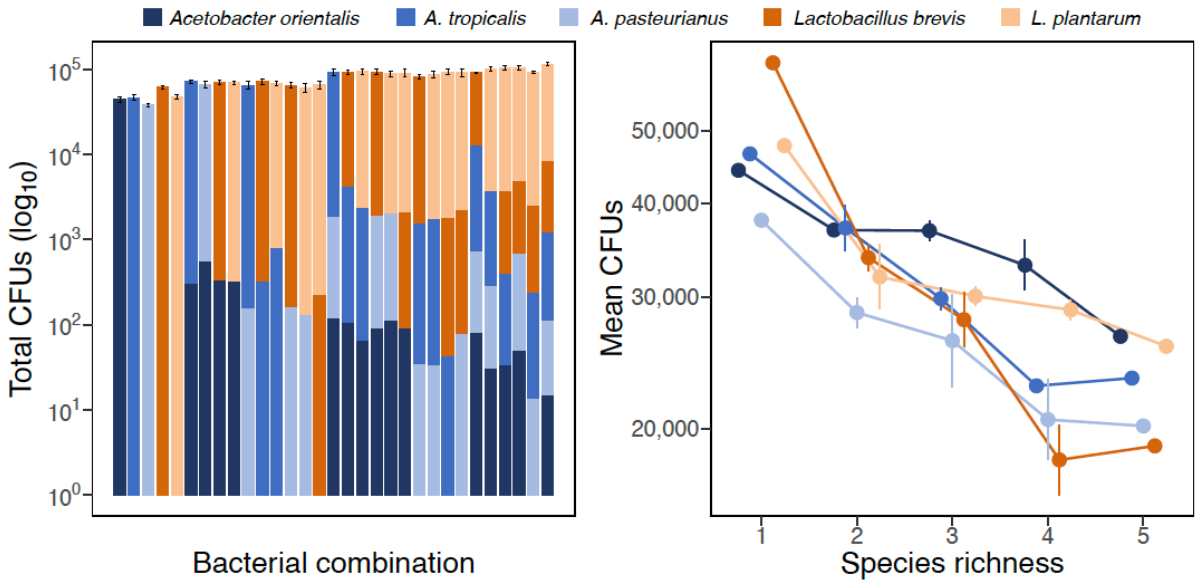

Supplementary Figure S9: Abundances of the different species (linear scale) for all 32 possible species combinations (N = 10 replicate flies per combination) with increasing species richness. The height of the bars in the left panel reflect the total microbial load ($\log_{10}$ scale), with the relative abundances of the constituent species shown by coloration (linear scale). Total increase in total bacterial load with increasing species richness is shown by increasing bar height from left to right. The right panel depicts the decline in species-specific colony-forming units (CFUs) counts in response to increasing species richness. All error bars show 95% confidence intervals.